Dynamic and steady-state behaviors of reverse saturable absorption in metallophthalocyanine

Chunfei Li, Lei Zhang, Miao Yang, Hui Wang, and Yuxiao Wang
Department of Physics, Harbin Institute of Technology, Harbin, 150001 China
(Received 23 March 1993)

The dynamic and steady-state processes of the reverse saturable absorption (RSA) and the related optical limiting (OL) and optical bistability (OB) in metallophthalocyanine have been studied in detail using rate equations and the light-propagation equation. The experiments for demonstrating RSA, OL, and OB in a copper phthalocyanine (CuPc) solution with a Q-switched, frequency-doubled neodymium-doped yttrium-aluminum-garnet (Nd:YAG) laser were accomplished. The experimental results were consistent with the dynamic theoretical simulations, also approximately in accordance with the expression of RSA derived from the same equations at the steady-state condition.

PACS number(s): 32.80.Rm, 33.80.Rv

I. INTRODUCTION

Nonlinear absorption means that the absorption coefficient of the medium depends on the light intensity. There are two kinds of nonlinear absorption: saturable absorption (SA), in which the absorption coefficient decreases with increasing light intensity, and reverse saturable absorption (RSA), in which the absorption coefficient increases with increasing light intensity.

As early as the 1960s, SA in various organic dyes were studied for with regard to laser pulse compression [1,2]. Most of the dispersive optical bistability (OB) studied extensively since 1975 was based on the mechanism of SA [3]. The origin of SA is due to the ground-state absorption of the medium, which can be described by a two-level model or a three-level model. During that time, the excited-state absorption was only considered as a "residual absorption" [4] or "unsaturable background absorption" which makes the pure absorptive optical bistability very difficult to realize [3].

Recently, RSA has been found in many organic materials [5–8], especially in molecules with a center-symmetric structure and the π-electron conjugated system. Metallophthalocyanine (MPc) is one of these materials, which usually exhibit SA at the peak of the ground-state linear absorption spectrum [9]; however, at the valley of the ground-state linear absorption spectrum, RSA could occur [10], because in this wavelength region the absorption cross sections of the excited-state are larger than that of the ground state. The RSA should be described by a multiple-level model. One of the important applications of RSA is in optical limiting for sensor and eye protection [11–15]. It also shows promise as a mirrorless pure absorptive OB [16].

Up until now, most works on RSA were experimentally demonstrated. Blau *et al.* [17,18] presented a set of rate equations describing a six-level model of the molecular system and a propagation equation to explain the RSA.

In this paper, we use a similar simplified theoretical model to simulate the steady-state and the dynamic behaviors of the RSA, the optical limiting (OL), and the absorptive OB in a MPc solution under the action of a laser pulse with different intensities and pulse widths. The theoretical simulations have been proved by the experimental results of RSA, OL, and OB in a copper phthalocyanine (CuPc) solution using a Q-switched neodymium-doped yttrium-aluminum-garnet (Nd:YAG) laser with an off-resonant wavelength of 532 nm.

The time-dependent transit transmission and populations of each energy level during an input laser pulse, the contributions of singlet (or doublet) and triplet (or quartet) excited states to RSA, and the effects of concentration and thickness of sample on OL are also discussed. The results of RSA, OL, and OB in this paper are suitable for all MPc's or other organic materials and are useful for designing optical limiters, absorptive optical bistable devices, and other photonic devices based on the excited-state nonlinear absorption.

II. ESTABLISHMENT OF THE THEORETICAL MODEL

The molecular structure of the MPc is shown in Fig. 1. It is a two-dimensional (2D) large molecule with symmetry D_{4h}. A center-metal atom or ion is connected with

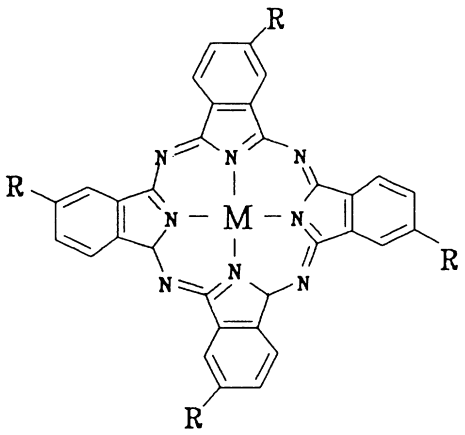

FIG. 1. The molecular structure of the MPc.

four ligands (the benzene ring plus the pyrrole ring) by nitrogen bridges. In MPc there are 18 π electrons surrounding the center metal with large delocalization to form a 2D π-electron conjugated system.

The energy-level diagram of the MPc is shown in Fig. 2. It has two energy-level systems: singlets (or doublets) and triplets (or quartets), in which S_1 is the ground state; S_2 and S_5 are the first excited state and an upper excited state in singlets (or doublets), respectively; S_3 and S_6 are the first excited state and an upper excited state in triplets (or quartets), respectively; and every electronic energy level involves many vibronic sublevels. Therefore, the incident photons with the same frequency can be simultaneously absorbed by molecules not only in the ground-state but also in both singlet (or doublet) and triplet (or quartet) excited states.

Figure 3 illustrates the ground-state linear absorption spectra for the CuPc in chloroform solution [10]. The AlPc-F (fluoroaluminum phthalocyanine) in pyridine solution and the GaPc-Cl (chlorogallium phthalocyanine) in pyridine solution have the same shape as the ground-state linear absorption spectrum [19]. In fact, all MPc's do have two similar ground-state absorption bands: the Q band in the 600–800 nm (visible) range and the B band in the 300–400 nm (near UV) range. The Q band is strongly dependent on the ligand (Pc ring); the different center metal causes it only a small change. In the region of 400–600 nm, the ground-state absorption of MPc's is very weak.

However, MPc has stronger excited-state linear absorption in the region of 400–600 nm. Figure 4 shows the transient different absorption spectra of MgPc (magnesium phthalocyanine) in dimethyl sulfoxide with a fluorescence lifetime of 7.5 ns and a triplet lifetime of 330 μs [20]. Curve 1, corresponding to the absorption of the first singlet (or doublet) excited state, is a difference spectrum between transition $S_2 \rightarrow S_5$ and transition $S_1 \rightarrow S_2$. Curve 2, corresponding to the absorption of the first triplet (or quartet) excited state, is a difference spectrum between transitions $S_3 \rightarrow S_6$ and $S_1 \rightarrow S_3$. Curve 3 is the ground-state absorption spectrum arising from the transition $S_1 \rightarrow S_2$. MPc's with different center metals have similar excited-state absorption spectra. From Fig. 4 we can see that all the maximums of the excited-state absorption are located on the wavelength around 500 nm, which is just the location of the minimum ground-state

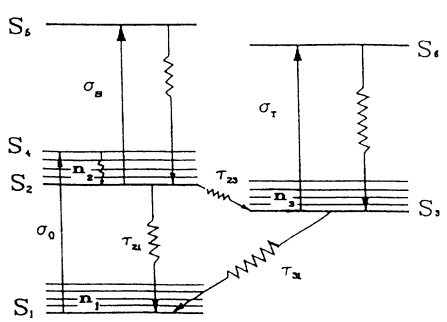

FIG. 2. The energy-level diagram of the MPc molecular.

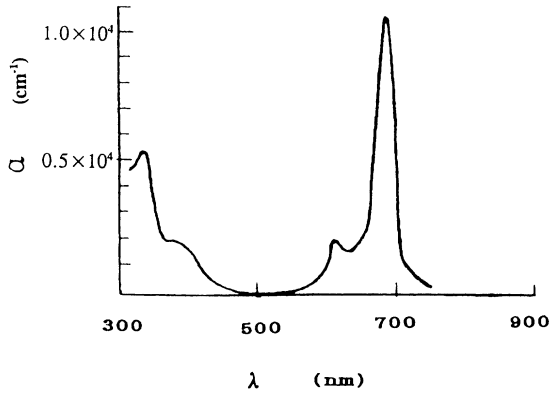

FIG. 3. The ground-state linear absorption spectra for CuPc in chloroform solution.

absorption. Therefore, the RSA in MPc's can be observed at this wavelength region.

The nonlinear absorption process of MPc can be described by a six-energy-level model, as shown in Fig. 1. Assuming the incident laser has a power density of $I(t)$, a pulse width of τ_L, and a nonresonant wavelength of 532 nm, the photons are absorbed by molecules in the ground state; this causes the transition of molecules from S_1 to a vibronic sublevel S_4 with an absorption cross section σ_0. Molecules in S_4 decay rapidly to S_2 with a lifetime of a few ps because of the overlap between vibronic sublevels, and most molecules quickly transit from S_2 to S_3 with a short nonradiative intersystem-crossing lifetime τ_{23}. The molecules in S_2 and S_3 can be exited to S_5 and S_6 with absorption cross sections σ_S and σ_T, respectively, by absorbing photons with the same wavelength of 532 nm. However, the lifetimes in S_5 and S_6 are extremely short (<1 ps). On the other hand, the molecules in S_2 partly return to the ground state by fluorescence emission or by the nonradiative transition with the lifetime τ_{21}, and the

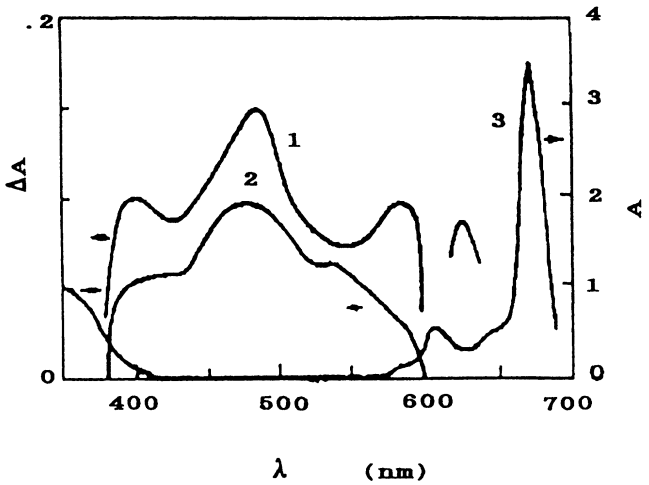

FIG. 4. The linear absorption spectra of MaPc in dimethyl sulfoxide: 1, the first triplet excited-state difference absorption spectrum; 2, the first singlet excited-state difference absorption spectrum; and 3, the ground-state absorption spectrum.

molecules in S_3 can also return to the ground state by phosphorescence emission or by the nonradiative transition with lifetime τ_{31}. But for most MPc solutions at room temperature, the fluorescence and the phosphorescence emissions are very weak and can be neglected.

In order to investigate quantitatively the nonresonant interaction between an incident laser light and a MPc molecular system with the six-level model, the following rate equation for describing the time variation of the population density in each energy level can be used:

$$\frac{d\mathbf{N}}{dt}=\hat{R}\mathbf{N}\ , \tag{1}$$

where $\mathbf{N}$ is a population vector matrix, which component expression is

$$\mathbf{N}=(n_1,n_2,n_3,n_4,n_5,n_6)\ ; \tag{2}$$

$\hat{R}$ is a rate operator with a 6×6 matrix,

$$\hat{R}=\begin{bmatrix} -\frac{\sigma_0 I}{h\nu} & 0 & \frac{1}{\tau_{21}} & \frac{1}{\tau_{31}} & 0 & 0 \\ 0 & \frac{1}{\tau_{42}} & -\frac{\sigma_S I}{h\nu}-\frac{1}{\tau_{21}}-\frac{1}{\tau_{23}} & 0 & \frac{1}{\tau_{52}} & 0 \\ 0 & 0 & \frac{1}{\tau_{23}} & -\frac{\sigma_T I}{h\nu}-\frac{1}{\tau_{31}} & 0 & \frac{1}{\tau_{63}} \\ \frac{\sigma_0 I}{h\nu} & -\frac{1}{\tau_{42}} & 0 & 0 & 0 & 0 \\ 0 & 0 & \frac{\sigma_S I}{h\nu} & 0 & -\frac{1}{\tau_{52}} & 0 \\ 0 & 0 & 0 & \frac{\sigma_T I}{h\nu} & 0 & -\frac{1}{\tau_{63}} \end{bmatrix}\ . \tag{3}$$

Because the lifetimes of energy levels S_5, S_6, and S_v are very short, the populations of these three levels can be neglected, and $\mathbf{N}$ and $\hat{R}$ can be reduced, respectively, to

$$\mathbf{N}=(n_1,n_2,n_3)\ , \tag{4}$$

$$\hat{R}=\begin{bmatrix} -\frac{\sigma_0 I}{h\nu} & \frac{1}{\tau_{21}} & \frac{1}{\tau_{31}} \\ \frac{\sigma_0 I}{h\nu} & -\frac{1}{\tau_{21}}-\frac{1}{\tau_{23}} & 0 \\ 0 & \frac{1}{\tau_{23}} & -\frac{1}{\tau_{31}} \end{bmatrix}\ . \tag{5}$$

The total nonlinear absorption coefficient α arises from the absorption of the ground state α_0 as a function of n_1, the absorption of the first excited singlet state α_S as a function of n_2, and the absorption of the first triplet state α_T as a function of n_3:

$$\begin{aligned}\alpha(t)&=\alpha_0(t)+\alpha_S(t)+\alpha_T(t)\\&=\sigma_0 n_1+\sigma_S n_2+\sigma_T n_3\ ,\end{aligned} \tag{6}$$

where n_1, n_2, and n_3 are functions of intensity I according to Eqs. (1), (4), and (5).

Considering that the variation of light intensity along the direction of light propagation (z) in the sample leads to a change in the absorption coefficient, we must established a light-propagation equation:

$$\frac{dI}{dz}=-(\sigma_0 n_1+\sigma_S n_2+\sigma_T n_3)I\ , \tag{7}$$

where I is a function of t and z.

The initial boundary conditions are

$$\begin{aligned}&n_1(t=-\infty,z)=N=n_1+n_2+n_3\ ,\\&n_2(t=-\infty,z)=n_3(t=-\infty,z)=0\ ,\\&I(t,z=0)=I_0 f(t)\ ,\end{aligned} \tag{8}$$

where N is the total population density, I_0 is the peak intensity of the incident laser, and $f(t)$ is a temporal function describing the pulse shape.

According to the difference in the response time to light, MPc's can be divided into two groups. Those in the first group, such as VOPc (vandadyl phthalocanine) and CuPc, with faster response times have short excited-state lifetimes τ_{23}, τ_{31}, and τ_{21}, because their center metals are paramagnetic metals or heavy-atom metals. Those in the second group, such as MgPc (magnesium phthalocyanine) and CAPc (chloroaluminum phthalocyanine), with slower response times have long lifetimes. Table I lists excited-state lifetimes τ_{23}, τ_{21}, and τ_{31} for the above

TABLE I. Excited-state lifetimes of the metallophthalocyanines.

Sample	τ_{23} (ns)	τ_{21} (ns)	τ_{31} (ns)
MgPc	59.0	14.7	500
CAPc	33.4	14.7	500
VOPc	<0.16	16.0	<20
CuPc	<0.15	14.8	<50

MPc's in air-equilibrated solutions at room temperature [1].

There are two kinds of theoretical methods: the steady-state theory and the dynamic theory. Which one could be used to deal with the RSA in a certain MPc molecular system? The answer depends on the comparison between the laser pulse width and excited-state lifetimes of the system. If the laser pulse width is much longer than all of excited-state lifetimes of the system, the steady-state theory can be used; if the laser pulse width is at least shorter than one of the excited-state lifetimes of the system, the dynamic theory should be used.

III. STEADY-STATE THEORY

When we use an incident laser with a pulse width τ_L longer than all the lifetimes of the MPc: τ_{23}, τ_{31}, and

$$\tau_2=(\tau_{23}^{-1}+\tau_{21}^{-1})^{-1}\approx\tau_{23}\ ,$$

the steady-state solution of Eqs. (1), (4)–(7) and (8) are

$$n_1=\frac{N}{1+\frac{I}{I_s}}\ , \tag{9}$$

$$n_2=\left[\frac{\tau_{23}}{\tau_{31}}\right]\left[\frac{I}{I_s}\right]\left[\frac{N}{1+\frac{I}{I_s}}\right]\ , \tag{10}$$

$$n_3=\left[\frac{I}{I_s}\right]\left[\frac{N}{1+\frac{I}{I_s}}\right]\ , \tag{11}$$

$$\alpha=\left[\frac{\sigma_0 N}{1+\frac{I}{I_s}}\right]\left[1+\frac{\sigma_S}{\sigma_0}\frac{\tau_{23}}{\tau_{31}}\frac{I}{I_s}+\frac{\sigma_T}{\sigma_0}\frac{I}{I_s}\right]\ , \tag{12}$$

where I_s is the saturable intensity which is defined as

$$I_s=\frac{h\nu}{\tau_{31}\sigma_0} \tag{13}$$

If $\sigma_S\sim\sigma_T$, $\tau_{23}\ll\tau_{31}$, α can be expressed as

$$\alpha=\alpha_0\left[\frac{1+KI'}{1+I'}\right]\ , \tag{14}$$

where $I'=I/I_s$ and $K=\sigma_T/\sigma_S$, $\alpha_0=\sigma_0 N$.

The plots of the absorption coefficient α versus the normalized incident peak intensity I_0/I_s for the different K are shown in Fig. 5, which shows that when $K>1$ ($\sigma_T>\sigma_0$) and α increases with increasing I, it exhibits RSA. However, when $K<1$ ($\sigma_T<\sigma_0$), α decreases with increasing I, it exhibits SA. In the off-resonant case, the ground absorption cross-section is very small, so it is easy to meet the condition of RSA $\sigma_T>\sigma_0$.

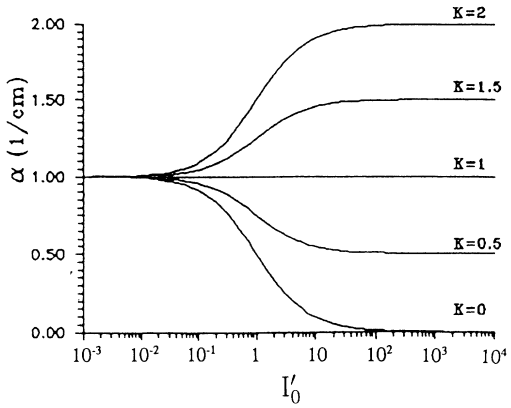

FIG. 5. Plots of the absorption coefficient of sample α versus the normalized incident peak intensity I_0/I_s for different $K=\sigma_T/\sigma_0$.

In an optically thick sample, the light intensity should be regarded as a function of the coordinate z along the direction of light propagation in the sample. Integrating both sides of Eq. (7) by using boundary conditions (8), we have

$$\int_{I_0}^{I_L}\left[\frac{1}{\alpha I}\right]dI=-\int_0^L dz\ . \tag{15}$$

Substituting Eq. (14) into Eq. (15), we get an analytical expression for RSA, i.e., the relation between the transmission and the incident intensity,

$$\ln\left[\frac{T}{T_0}\right]=\left[1-\frac{1}{K}\right]\ln\left[\frac{1+KTI_0'}{1+KI_0'}\right]\ , \tag{16}$$

where $T=\exp(-\alpha L)$ is the nonlinear transmission, $T_0=\exp(-\alpha_0 L)$ is the linear transmission and $I_0'=I_0/I_s$ is the normalized incident peak intensity to the saturable intensity. If taking $T_0=0.60$, $I_s=2\times10^7$ W/cm^2 for

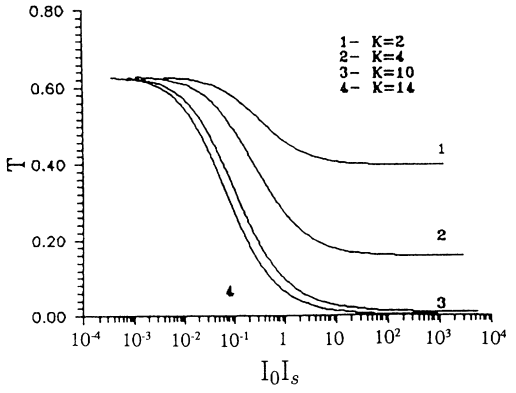

FIG. 6. Characteristics of RSA in steady state: The transmission of the sample T versus the normalized intensity for $K=\sigma_T/\sigma_0=2$, 4, 10, and 14.

$K=2$, 4, 10, and 14, we get a set of the T-I_0 curves as shown in Fig. 6. One can see that the RSA of MPc with a larger K is stronger than that of MPc with a smaller K.

IV. DYNAMIC ANALYSIS

Now we begin to study the RSA dynamic process in MPc by using the dynamic equations in Sec. II. As a sample, we select a CuPc molecular system with fast intersystem-crossing time. Because the unpaired Cu d electron is weakly coupled to singlets and triplets of a molecule, it makes the singlets become doublets (^2S) and the triplets split into triplet-doublets (^2T) and quartets (^4T) [21]. Triplet-doublets are combined with doublets to form a same energy-level system. The lowest triplet-doublet state can be regarded as S_2 and the lowest quartet can be regarded as S_3 in our six-level model. The data for dynamic simulation of RSA in CuPc solution are mainly taken from Ref. [1], in which the lifetime τ_{31} depends on two effects: the annihilation reaction [22] due to the concentration of solution and the quenching effect due to the oxygenation of solution. In addition, the CuPc solution sample used in our experiment has a thickness of 0.5 cm and a concentration $7.5\times10^{-4}M$, which is larger than the value in Ref. [1], and the solution is air equilibrated at room temperature, so the τ_{31} is estimated at 10 ns. The value of σ_S is also taken from our experimental results (see Sec. V). Accordingly, the data for the CuPc sample at a wavelength of 532 nm are listed in Table II.

The light source we used is a laser with a nonresonant wavelength $\lambda=532$ nm and with two pulse widths $\tau_L=15$ ns ($>\tau_{23}$) and $\tau_L=80$ ps ($<\tau_{23}$), respectively. Assume that the light intensity is a Gaussian function of the time

$$I(t,z)=I_0(z)\exp[-c(t/\tau_L)^2],$$

where I_0 is the peak intensity at z and c is the normalized constant.

Substituting all of the data into Eqs. (1), (4)–(7), and boundary conditions (8), and calculating numerically via computer, we have obtained the following dynamic simulated results of RSA.

A. Time-dependent populations during a light pulse

Figure 7 illustrates the curves of populations n_1, n_2, and n_3 versus the time during a single light pulse under two different input fluences: (1) $F_0=0.1$ J/cm^2 and (2) $F_0=1$ J/cm^2, with a pulse width of 15 ns. From Fig. 7 we can see that when the input fluence F_0 is smaller (at 0.1 J/cm^2), most molecules are populated in the ground-state, but when the F_0 increase until 1 J/cm^2, most molecules will be populated in the first quartet excited state

TABLE II. The experimental data of CuPc solution.

Absorption cross section (cm^2)		Relaxation time (ns)	
σ_0	2.0×10^{-18} cm^2	τ_{S0}	15
σ_S	3.5×10^{-17} cm^2	τ_{T0}	10
σ_T	2.6×10^{-17} cm^2	τ_{ST}	0.15

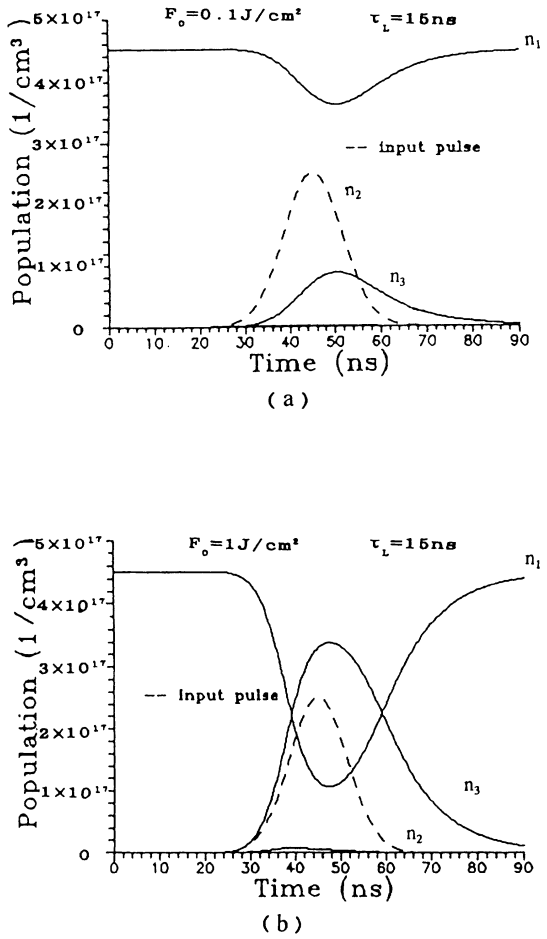

FIG. 7. Populations in S_0, S_1, and T_1 versus the time during a single light pulse with a width of 15 ns under two input fluences: (1) $F_0=0.1$ J/cm^2 and (2) $F_0=1$ J/cm^2.

(or the triplet state) S_3. In this case the RSA can be observed.

B. Contributions of each energy level to nonlinear absorption

In order to study the contributions of each energy level to nonlinear absorption, we have calculated curves of the absorbed light intensity of molecules in each level, $\alpha_0 I$, $\alpha_S I$, and $\alpha_T I$, versus the time during a single laser pulse under two different input fluences: (1) $F_0=0.1$ J/cm^2 and (2) $F_0=1$ J/cm^2. Figures 8 and 9 correspond to different pulse widths: $\tau_L=15$ ns and 80 ps, respectively. When the input fluence is smaller (at 0.1 J/cm^2), the contribution of the ground state is dominant in both cases; it exhibits SA. When the input fluence become larger until 1 J/cm^2, the contribution of the excited-state absorption will be more important; it causes RSA to occur. If $\tau_L>\tau_{23}$, the contribution of level S_3 to RSA is dominant, but if $\tau_L<\tau_{23}$, the contribution of level S_2 to RSA is dominant.

C. Transient transmission versus time during a light pulse

Figure 10 shows the curves of the transient intensity transmission $T(t)=I(t,L)/I(t,0)$ versus the time during

a single laser pulse under $F_0=0.1$ J/cm^2, 0.1 J/cm^2, and 1 J/cm^2. The data of the sample are $C=7.5\times10^{-4}M$ and $L=0.5$ cm. The data of the laser are $\lambda=532$ nm and $\tau_L=15$ ns. Assume that the power density is a Gaussian function of time. The curves show that the transmission decreases with an increase in the input intensity and increases with a decrease in the input intensity during the laser pulse. In addition, the RSA effect becomes stronger with an increase in the input fluence.

D. Characteristics of reverse saturable absorption

The characteristics of RSA can be also described by the energy transmission $T=F_L/F_0$ versus the time, where $F_0=F(0)$ and $F_L=F(L)$ are input fluence and output fluence, respectively. A dynamic simulation of RSA in CuPc solution, the transmission versus input fluence, as shown in Fig. 11 (see the solid curve). It fits in experimental results very well, better than the simulation of the expression (16) for the steady-state (the dash curve). The steady-state condition is approximately to be met because of the laser power-width we used ($15ns$) is close to the lifetime $\tau_{31}=10ns$.

E. Material-dependent characteristics of optical limiting

The theoretical characteristics of optical limiting in CuPc is shown in Fig. 12, in which 1 is a dynamic simulation (solid curve) which is in good accordance with experimental results and 2 is a steady-state simulation (dashed curve) which approximately fits the experimental results. Figure 13 shows the curves of the output fluence versus the input fluence for different ratios $K=\sigma_T/\sigma_0=2$, 4, 10, and 14. It is obvious that the material with larger K has stronger RSA and then has better OL. Generally, MPc has better OL as compared with C_{60} because for MPc, $K>10$; for C_{60}, $K\sim3$ [22,23].

For a material, there are different OL characteristics for different wavelengths or pulse widths of the laser, because different wavelengths or pulse widths lead the ratio K of material to be different.

In order to understand the effect of thickness and concentration of the material on the RSA, we have calculated two groups of curves of optical limiting as shown in Fig. 14: Curve 1 shows the output fluence versus input fluence for different thicknesses $L=0.1$, 0.5, and 1 cm, with the same concentration $C=7.5\times10^{-4}M$; Curve 2 shows the output fluence versus the input fluence for

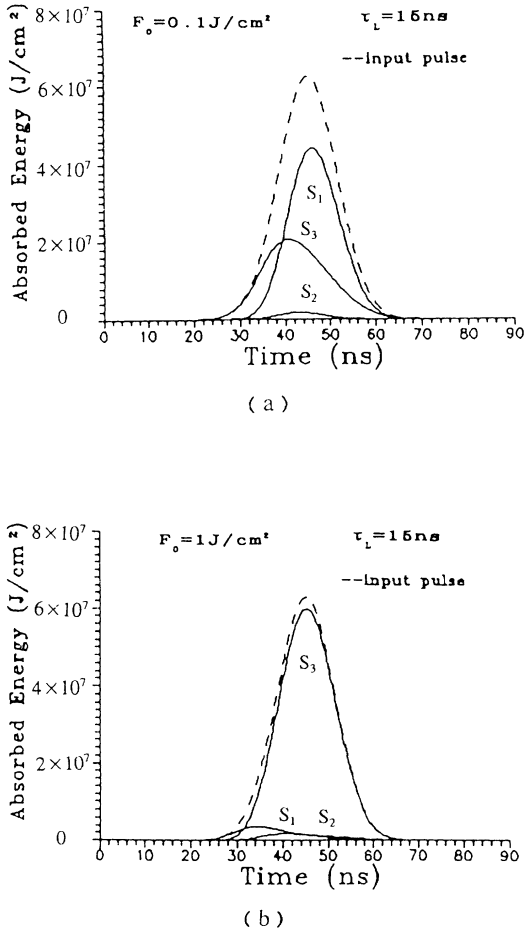

FIG. 8. Absorbed light intensities of molecules in S_0, S_1, and T_1 versus the time during a single laser pulse with a width of 15 ns under two input fluences: (1) $F_0=0.1$ J/cm^2 and (2) $F_0=1$ J/cm^2.

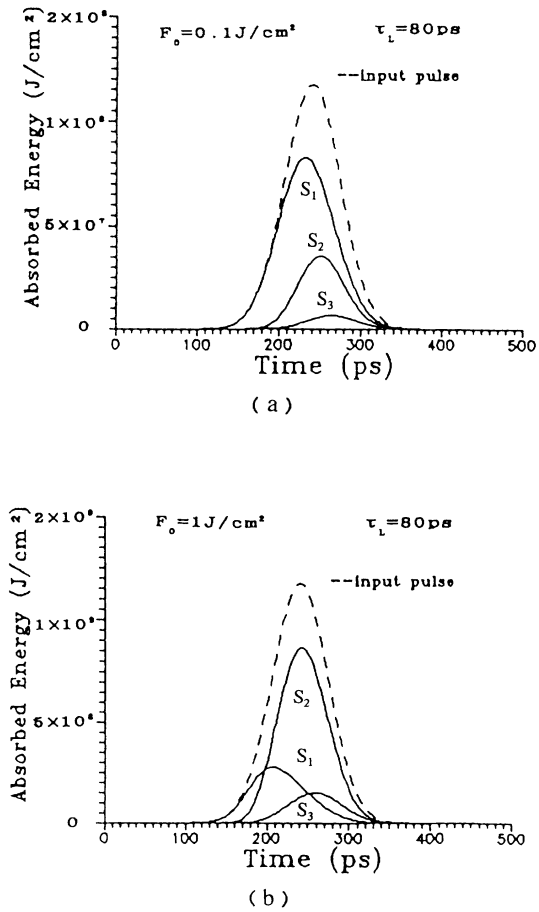

FIG. 9. Absorbed light intensities of molecules in S_0, S_1, and T_1 versus the time during a single laser pulse with a width of 80 ps under two input fluences: (1) $F_0=0.1$ J/cm^2 and (2) $F_0=1$ J/cm^2.

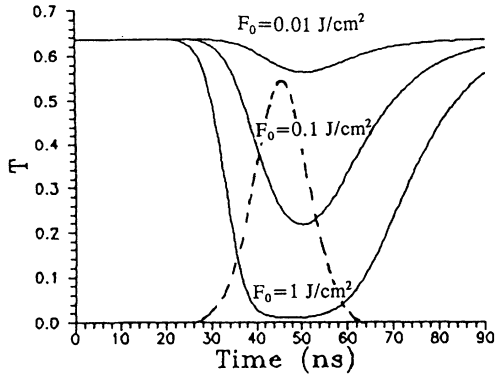

FIG. 10. Transient transmissions versus the time during a single laser pulse with a width of 15 ns under three different input fluences: $F_0=0.01$, 0.1, and 1 J/cm^2.

different concentrations $C=3.8\times10^{-4}M$, $7.5\times10^{-4}M$, and $1.5\times10^{-4}M$, with the same thickness $L=0.5$ cm. We can see that the sample with larger L or larger C has better characteristics of OL—for example, the saturable threshold of output fluence is only 0.4 J/cm^2 for the sample with $L=1$ cm or $C=1.5\times10^{-3}M$. However, the linear transmission of this sample is too low—only 0.4. The desirable transmission for an ideal OL device is required to be $\geq 70\%$; therefore, it is necessary to make a tradeoff between the transmission and the concentration or thickness of the material.

F. Absorptive mirrorless transient optical bistability

With a laser source of $\tau_L=15$ ns, $\lambda=532$ nm, and $F_0=1$ J/cm^2, we obtained by simulation the optical bistability as shown in Fig. 15: Curve 1 is the output intensity $I(t,L)$ and the input intensity $I(t,0)$ versus the time and curve 2 is the corresponding curve of output $I(t,L)$ as a function of the input $I(t,0)$. The wave form of the output intensity is in advance of the wave form of the input intensity, and the hysteresis loop exhibits a transient increasing optical bistability caused by the absorption and the relaxation of the excited state, which is a pure electronic process with ns or ps switching time. The switching time depends on the input pulse width and the lifetime of the excited state. We should also mention that it is a mirrorless absorptive OB.

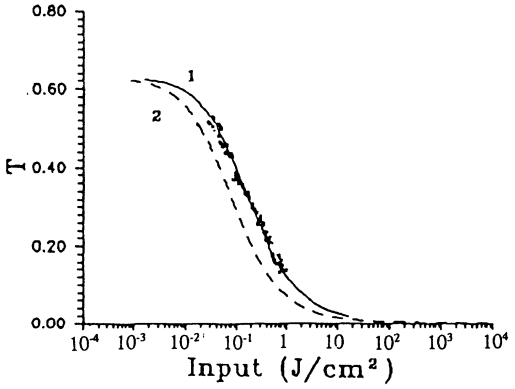

FIG. 11. Theoretical simulations for the RSA in a CuPc solution: the transmission versus the input fluence. The solid curve (1) is the dynamic simulation; the dashed curve (2) is the steady-state simulation. The comparison with experimental data is also shown.

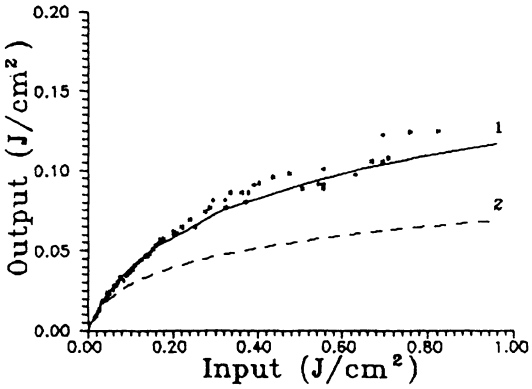

FIG. 12. Theoretical simulations for OL in a CuPc solution: the output fluence versus the input fluence. The solid curve (1) is the dynamic simulation; the dashed curve (2) is the steady-state simulation. The comparison with experimental data is also shown.

V. COMPARISON: EXPERIMENT AND THEORY

The sample used in our experiment was a CuPc in chloroform solution with a concentration of $7.5\times10^{-4}M$ and was placed in a cell with a practical thickness of 0.5 cm. The linear transmission of the sample T_0 is 0.63.

In order to get RSA at nonresonance, a Q-switched, frequency-doubled Nd:YAG laser with a pulsewidth of 15 ns at wavelength $\lambda=532$ nm was employed as the light source. The input and output pulse energies and average powers were measured by photodetectors, and the pulse shapes were recorded by a Tek 7934 storage oscilloscope.

From the experimental data of the input fluence and the output fluence, we got a group of experimental dots as shown in Fig. 11, which have proved the correctness of

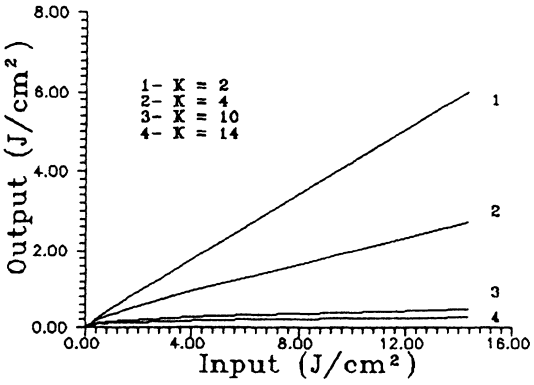

FIG. 13. Characteristics of optical limiting in a CuPc solution, the output fluence versus the input fluence, for $K=\sigma_T/\sigma_0=2$, 4, 10, and 14.

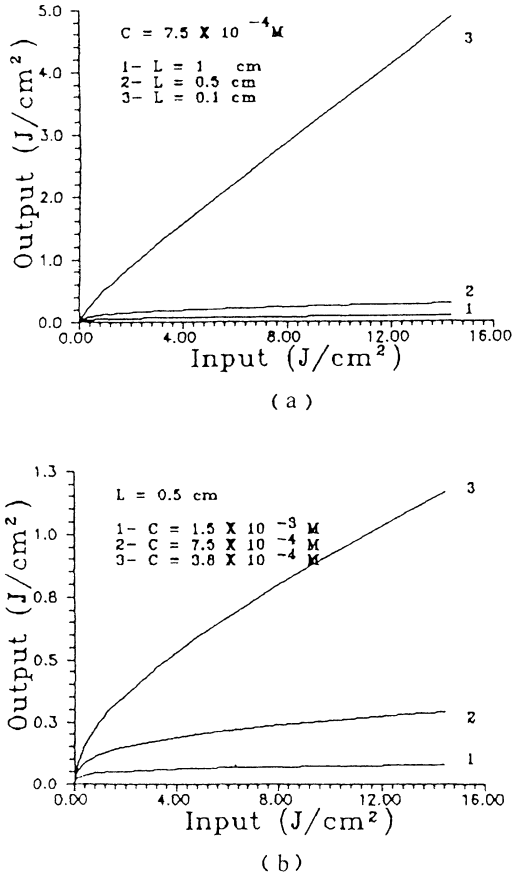

FIG. 14. Characteristics of optical limiting in a CuPc solution: (1) For a concentration of $7.5\times10^{-4}M$ and different thicknesses $L=0.1$, 0.5 and 1 cm and (2) for a thickness of 0.5 cm and different concentrations $C=3.8\times10^{-4}M$, $7.5\times10^{-4}M$, and $1.5\times10^{-4}M$.

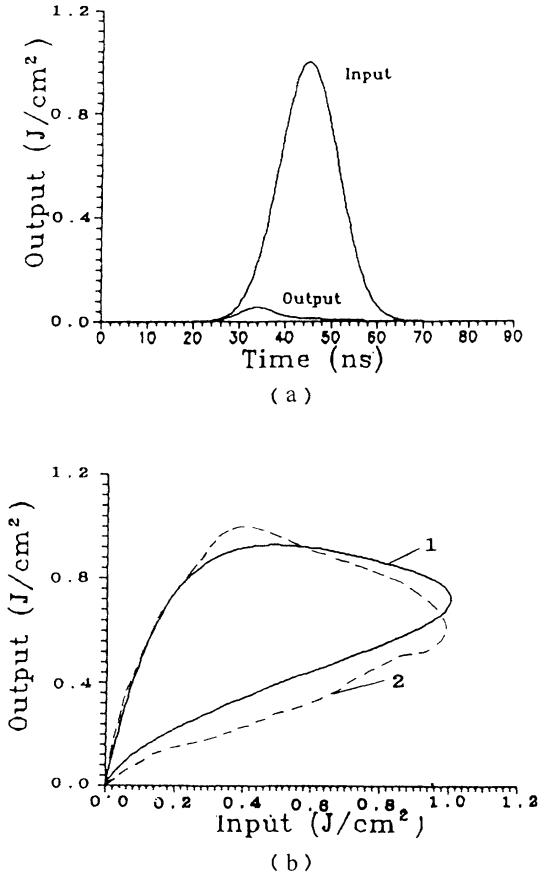

FIG. 15. Optical bistability in a CuPc solution when the laser with $\tau_L=15$ ns, $\lambda=532$ nm, and $F_0=1$ cm^2: (1) The output intensity and the input intensity versus the time and (2) the output intensity as a function of the input intensity, in which 1 is a theoretical curve of OB and 2 is a corresponding experimental curve of OB.

our dynamic theoretical model and the steady-state expression for RSA in CuPc when we selected $K=13$ for the CuPc solution in our experimental condition. We also found that the RSA in CuPc solution appears in the region of input influence from 10 mJ/cm^2 to 10 J/cm^2.

The experimental results of OL and OB are also in good accordance with our dynamic analysis as shown in Figs. 12 and 15(b), respectively.

VI. CONCLUSION

In this paper we have systematically studied the dynamic and the steady-state behaviors of the RSA in MPc using CuPc as a sample. The influences of both material and laser parameters on RSA and OL are also analyzed. The theoretical simulations agree well with the experimental results.

The RSA is due to the excited-state nonlinear absorption which is one of the excited-state nonlinear optics phenomena. According to the K-K relation, the excited-state nonlinear dispersion and the excited-state polarization should also be taken into account. Therefore, the investigation of RSA will open a new field of nonlinear optics—"excited-state nonlinear optics."

The RSA is a pure electronic process; it could be applied to design a series of new photonic devices, such as optical switches, optical logics, optical memories, optical limiters, optical modulators, and so on. These kinds of photonic devices have advantages of fast response (nanoseconds to subpicoseconds), low liner absorption, and mirrorless structure [24]. It might be possible to use them in optical communication, optical computing, and sensor protection.

The RSA in MPc has been discussed in detail in this paper. In comparison with other materials, MPc has better RSA characteristics because of its large ratio K — for example, for C_{60}, $K=3$ [17], but for CuPc, $K>10$. The best RSA property in MPc appears in the visible wavelength range around 500 nm, so the common frequency-doubled Nd:YAG laser with short pulse can be used as a light source.

In conclusion, MPc is a promising material for application in photonic devices based on RSA. But in order to optimize the device we need solid MPc materials (crystals and thin films) with a high damage threshold, large ratio K, and other good properties. Therefore, it is necessary to improve the chemical structure of MPc.

[1] M. Hercher, W. Chu, and D. L. Stockman, IEEE J. Quantum Electron. **QE-4**, 954 (1968).
[2] W. F. Kosonocky and S. E. Harrison, J. Appl. Phys. **37**, 4789 (1966).
[3] H. M. Gibbs, *Optical Bistability: Controlling Light with Light* (Academic Press, New York, 1985).
[4] W. E. K. Gibbs, Appl. Phys. Lett. **11**, 113 (1967).
[5] R. Adair, L. L. Chare, and S. A. Payne, J. Opt. Soc. Am. B **4**, 875 (1987).
[6] R. C. Hoffman, K. A. Stetyick, and R. S. Potember, J. Opt. Soc. Am. **6**, (1989).
[7] L. W. Tutt and S. W. McCahon, Opt.Lett. **15**, 700 (1990).
[8] D. G. McLean, R. L. Sutherland, M. C. Brand, D. M. Brandelik, P. A. Fleitz, and T. Pottenger, Opt. Lett. **11**, 858 (1993).
[9] Z. Z. Ho and N. Peyghambarian, Chem. Phys. Lett. **148**, 107 (1988).
[10] Chunfei Li, Hui Wang, Miao Yang, Lei Zhang, and Yuxiao Wang, Acta Opt. Sin. **13**, 219 (1993).
[11] R. C. Hoffman, K. A. Stetylck, R. A. Potember, and D. G. Mclean, J. Opt. Soc. Am. B **6**, 772 (1989).
[12] D. R. Coulter, V. M. Miskowski, J. W. Perry, T. Wei, E. W. Van Stryland, and D. J. Hagan, Proc. Soc. Photo-Opt. Instrum. Eng. **1105**, 42 (1989).
[13] S. W. McCahon, L. W. Tutt, M. B. Klein, and G. C. Valley, SPIE Proc. **1307**, 304 (1990).
[14] L. W. Tutt and A. Kost, Nature **356**, 225 (1992).
[15] A. Kost, L. Tutt, M. B. Klein, T. K. Dougherty, and W. E. Elias, Opt. Lett. **5**, 334 (1993).
[16] S. Speiser and K. L. Chisena, Appl. Phys. B **45**, 137 (1988).
[17] W. Blau, H. Byrne, and W. M. Dennis, Opt. Commun. **56**, 25 (1985).
[18] F. Henari, J. Callaghan, H. Stiel, W. Blau, and D. J. Cardin, Chem. Phys. Lett. **12**, 144 (1992).
[19] Z. Z. Ho, C. Y. Ju, and W. M. Hetherington III, J. Appl. Phys. **62**, 116 (1987).
[20] Hiroyuki Ohtanl, Takayoshi Kobayashi, Takeshi Ohno, Shunji Kato, Takashi Tanno, and Akira Yamada, J. Phys. Chem. **88**, 18 (1984).
[21] P. S. Vincett, E. M. Voigt, and K. E. Rieckhoff, J. Chem. Phys. **55**, 4131 (1971).
[22] T. W. Ebbcsen, K. Tanigaki, and S. Kuroshima, Chem. Phys. Lett. **181**, 501 (1991).
[23] Chun-Fei Li, Yu-Xiao Wang, Feng-Yun Guo, Rui-Bo Wang, and Lei Zhang, Acta Phys. Sin. **42**, 1236 (1993).
[24] Chun-fei Li, Miao Yang, Fengyun Guo, Yuxiao Wang, and Kunu Tada, Int. J. Nonlinear Opt. Phys. (to be published).